Proceedings of the ECCOMAS Thematic International Conference on Simulation and Modeling of Biological Flows (SIMBIO 2011) September 21–23, 2011, VUB, Brussels, Belgium

Numerical Prediction of Hemolysis Based on Computational Fluid Dynamics

Hai Yu*, Dominique Thévenin, Gábor Janiga

Institut für Strömungstechnik und Thermodynamik,
Fakultät für Verfahrens- und Systemtechnik,
Otto-von-Guericke-Universität Magdeburg,
Universitätsplatz 2, D-39106 Magdeburg, Germany
hyu@st.ovgu.de thevenin@ovgu.de janiga@ovgu.de
*: Corresponding author

Abstract

The computational prediction of hemolysis based on Computational Fluid Dynamics (CFD) is considered in the present work. Hemodynamics is computed by relying on ANSYS software and coupled with a postprocessing based on Matlab. The purpose of the project is to develop a reliable CFD-based technique to predict hemolysis in medical equipments, especially blood pumps, that will be ultimately included into an automatic optimization process for the design of improved blood-pump geometries.
Keywords: hemolysis, computational fluid dynamics, shear stress, strain, FDA critical path, sudden expansion.

Introduction

1. Background Information

Our research group has a long experience on flow optimization associated to Computational Fluid Dynamics [1]. This coupled approach, denoted in what follows CFD-O (CFD-based Optimization) has been in particular applied to the design optimization of a variety of turbomachines (see for instance [2,3] for recent results). The developed, automatic optimization method is carried out by coupling an in-house optimization library (called OPAL) with a simulation code for Computational Fluid Dynamics (CFD). In the present project, CFD relies on the ANSYS-CFX code. CFD-O based on the coupling between OPAL and CFX will ultimately be applied to optimize the 3D geometry of a single-stage axial blood pump, considering after a thorough literature analysis that this is the most promising concept for future applications.

CFD-O and more generally optimization can only be carried out when suitable objectives have been identified. In the present case, the power coefficient measuring the efficiency of the system will be retained as one objective, as usually done in the optimization of turbomachines. However, it is clear that the level of hemolysis is of paramount importance for a human blood pump. It will therefore be retained as well as objective, leading to a concurrent optimization involving two, probably contradictory objective functions.

At the difference of previous projects in our group like [2,3], it is therefore necessary to develop a suitable and reliable procedure to derive the hemolysis level from the CFD results. A dedicated Matlab code has been developed to meet this purpose. It reads all required data from the CFX-Post output file, and after finishing post-processing feeds back the hemolysis result to the optimizer, OPAL. The finally resulting computational loop is presented in Fig.1 and involves 4 coupled tools: ICEMCFD for geometry and mesh generation, CFX for the flow simulation, Matlab for the post-processing as well as for preparatory steps to initialize derived geometries, and finally OPAL for the external optimization loop, calling all the other simulation tools in the right sequence.

Before starting CFD-O, it is absolutely essential to validate in an appropriate manner all the involved models and procedures. This applies in particular in the present case to the hemolysis model. The FDA critical path project provides valuable flow properties and hemolysis data for an 18 cm long tube with sudden expansion. These results have been retained as validation benchmark for the developed Matlab code, as described in the rest of this paper.

2. Numerical Prediction of Hemolysis.

After analyzing the scientific literature on this subject, the tensor-based blood-damage model documented in [4,5] has been retained for the present work. In this model, a red blood cell is regarded as similar to a droplet in a flow. Its shape and orientation are represented by a symmetric, positive-definite 3d-order morphology tensor S_n. The evolution of S_n occurs subject to four effects:

1. resistance to deformation and rotation: $-(S_n -$

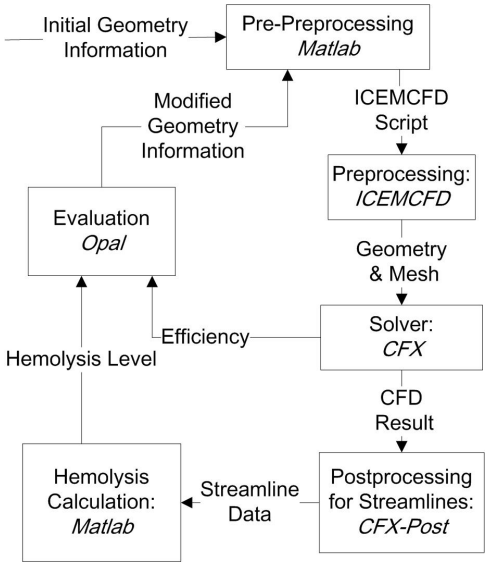

Figure 1 Flow chart of the optimization method and employed computational tools.

$g(S_n)I)$;

2. shear-induced deformation: $\tilde{\varepsilon}_n \cdot S_n + S_n \cdot \tilde{\varepsilon}_n$;
3. shear-induced rotation: $\tilde{W}_n \cdot S_n + S_n \cdot \tilde{W}_n$;
4. and rotation of the surrounding frame: $\Omega_n \cdot S_n + S_n \cdot \Omega_n$.

Combining all four contributions together with efficiency factors f_1, f_2, f_3 for the first three terms, one obtains finally following equation to describe the evolution of S_n with time t:

$$\begin{aligned}\triangle S_n = \big(&- f_1[S_n - g(S_n)I] + f_2[\tilde{\varepsilon}_n \cdot S_n + S_n \cdot \tilde{\varepsilon}_n] \\ &+ f_3[\tilde{W}_n \cdot S_n + S_n \cdot \tilde{W}_n] + [\Omega_n \cdot S_n + S_n \cdot \Omega_n]\big) \triangle t\end{aligned} \quad (1)$$

where, $\tilde{\varepsilon}_n = (1/2)(\nabla u + \nabla u^T)$ is the (symmetric) strain tensor of the flow; $W_n = (1/2)(\nabla u - \nabla u^T)$ is the (anti-symmetric) vorticity tensor of the flow; $\tilde{W}_n = W_n - \Omega_n$ is the vorticity really encountered by the droplet in its own frame of reference; $\Omega_n = \tilde{e_i}(\frac{\partial \tilde{e_i}}{\partial t} + u \bullet \nabla \tilde{e_i})$ is the rotation rate of the frame of reference; and $g(S_n) = 3III/II$, with $III = (\mathrm{tr}(S_n))^2 - \mathrm{tr}(S_n^2)$, $II = \det(S_n)$. When solving this equation in practice, Ω_n is considered at iteration n to be the rotation rate of the previous time step, $n-1$:

$$\Omega_n = (e_i)_n \frac{(e_i)_n - (e_i)_{n-1}}{\triangle t} \quad (2)$$

where, $(e_i)_n$ refers to eigenvectors of S_n. Hemolysis is finally calculated by Eq.(3):

$$\frac{\triangle H_b}{H_b} = 3.63\ 10^7 \left(\mu \sqrt{\frac{f_1^2 \varphi^2}{(1-\varphi^2) f_2^2}} \right)^{2.416} t^{0.785} \quad (3)$$

where, $\varphi = (L-B)(L+B)$, refers to the instantaneous aspect ratio of the droplet, denoting L the longer length (semi-major axis) contained within the droplet, and B its shorter length (semi-minor axis).

In this strain-based model, the deformation level is not directly proportional to the shear rate at the same instant in time, but is determined by the history of stress encountered by the blood cell and corresponding accumulation of constraints. Beyond a certain threshold, hemolysis is then directly and positively correlated to shape deformation.

Numerical Methods for Validation of Hemolysis Model

1. Main steps

In order to check the validity of the model implemented in Matlab, four steps are necessary:

i Generate corresponding geometry and mesh, which is done using ICEMCFD.
ii Solve the considered flow by CFD, which is done using ANSYS.
iii Extract the pathlines of the obtained steady flow solution using CFX-Post to export velocity magnitude, position vector and velocity gradient matrix at each point along the pathlines to one data file.
iv Import the pathline data into Matlab, and use the previously described strain-based algorithm to calculate the associated rate of hemolysis.

Finally, the obtained results can be compared with published results to assess their validity.

2. CFD Simulation

The tube with a sudden expansion employed for the FDA Critical Path project has been retained to validate the hemolysis prediction method [6].

Figure 2 Tube with sudden expansion used for the FDA Critical Path project [6], with blood flow from left to right.

Four different flow conditions have been tested, as listed in Table 1.

Table 1 Considered flow conditions

Flow rate (m^3/s)	$5.21\ 10^{-6}$	$3.64\ 10^{-5}$	$5.21\ 10^{-5}$	$6.77\ 10^{-5}$
Reynolds number	500	3 500	5 000	6 500
Flow state	Laminar	Turbulent	Turbulent	Turbulent

As boundary condition, a parabolic velocity profile has always been applied at the inlet for each flow rate. After many tests and an analysis of the relevant conditions, the Transition SST model has been systematically employed as turbulence model during these simulations based on the RANS (Reynolds Averaged Navier-Stokes) approach. Blood is represented as a viscoelatic fluid. The Carreau-Yasuda viscosity model has been systematically applied in

the CFD simulation. In this model, fluid viscosity η varies with shear rate γ.

$$\eta = \eta_\infty + (\eta_0 - \eta_\infty)[1 + \gamma^2\lambda^2]^{(n-1)/2} \qquad (4)$$

where, λ is the time constant, n is the power-law index, η_0 and η_∞ are, respectively, the zero- and infinite-shear viscosities. The employed parameters are listed in Table 2.

Table 2 Parameters employed for Carreau-Yasuda Model

λ	n	η_0	η_∞
s	-	kg/m.s	kg/m.s
10.3	0.35	0.063	0.0047

3. Hemolysis

As explained previously, the deformation of the red blood cells is computed along pathlines extracted after convergence of the steady-state CFD simulation. Hemolysis happens when the red blood cell distortion induced by the temporal accumulation of shear stress has reached a given threshold. Beyond that threshold, the membrane of the red blood cell begins to crack and hemoglobin leaks out. Hemolysis is calculated first along each pathline separately, using the method depicted in Fig.3. Then, global hemolysis is achieved by computing a mean value from all pathlines weighted by the associated flow-rate in order to take into account the fact that not all pathlines will transport statistically the same number of blood cells. For each configuration, 869 pathlines have been extracted, always choosing the starting position of the pathlines as being equally spaced along the inflow surface. In this manner, all pathlines behave identically at the very beginning of the computational domain, but obviously differ due to the different flow conditions obtained later as a function of the flow-rate.

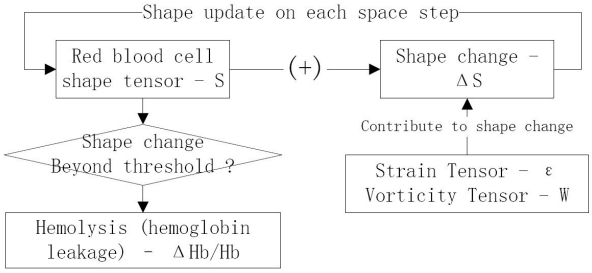

Figure 3 Iteration carried out along each pathline separately.

Results

1. CFD result for blood flow

A brief comparison between our CFD results concerning the velocity profile along the centerline and two series of experimental results published in [6,7] is illustrated in Fig.4. Please note that the y-scale (i.e., the peak velocity) widely differ for each subfigure. As a whole the agreement appears to be very fair at all Reynolds numbers, with noticeable differences visible only locally just after the sudden expansion. The observed discrepancies are similar to the differences found between the two measurement campaigns for the same experimental conditions (red squares vs. blue diamonds). We feel therefore confident that the main flow features are reproduced accurately with the employed CFD model and the underlying, quite fine 3D structured mesh, containing about 3.5 million volume elements.

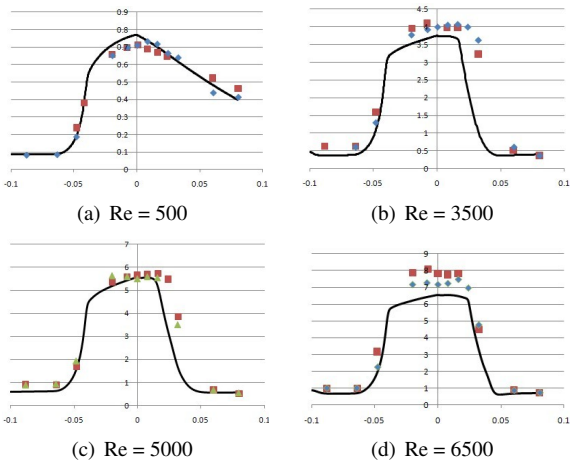

Figure 4 Comparison of our CFD results (lines) with two independent experimental measurement campaigns (red square and blue diamond) concerning the centerline velocity profile.

2. Pathline extraction

Selected pathlines extracted for all four Reynolds numbers at the same starting points along the inlet plane are shown in Figs.5 to 8. A striking feature is that a large and strong recirculation region is observed after the sudden expansion at a Reynolds number of 5 000 (Fig.7) and even more so for Re= 6 500 (Fig.8). On the other hand, no recirculation is visible at all at Reynolds number 500 and 3 500 when following the fluid particles entering through the inlet. Looking at Fig.5, the fluid near the wall after the sudden expansion does not interact with the flow entering from the inlet.

Figure 5 Selected pathlines from inlet for Re = 500

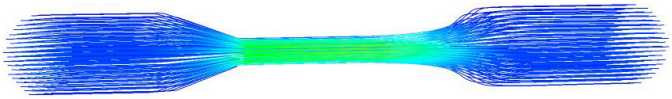

Figure 6 Selected pathlines from inlet for Re = 3 500

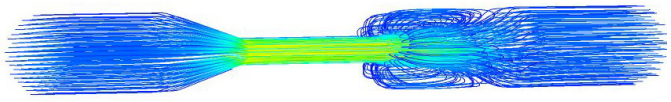

Figure 7 Selected pathlines from inlet for Re = 5 000

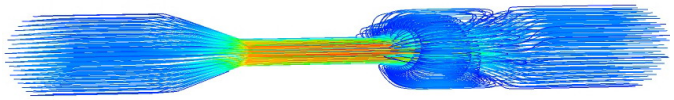

Figure 8 Selected pathlines from inlet for Re = 6 500

3. Hemolysis Prediction

The parameters f_1, f_2, f_3 determine the strength of the different processes finally leading to hemolysis. Clearly, there is quite a large uncertainty concerning the corresponding values, and different parameter combinations lead to widely varying results concerning hemolysis prediction. Figure 9 corresponds to the published results obtained within the framework of the FDA Critical Path initiative. For these results, the hemolysis obtained for a Reynolds number of 5 000 is used as a reference to normalize all other values.

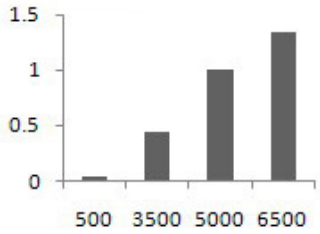

Figure 9 Relative hemolysis index choosing the case with Re=5 000 **as reference (index = 1) as measured by FDA during the Critical Path project [8,9].**

Figure 10 illustrates the large variations obtained when varying the prefactors f_1 to f_3. The first subfigure (a) corresponds to the set of parameter values recommended in [4]. It can be easily noticed that the choice of the prefactors f very strongly impacts the results. Using the parameter values from [4], the results of the numerical predictions do not coincide at all with the published evolution and show no clear trend when varying the Reynolds number. Using a manual trial-and-error procedure, it is readily possible to identify other parameter values leading to a considerably better agreement with the experimental measurements. From all combinations tested up to now, the values $f_1 = 0.0115$, $f_2 = 0.005$ and $f_3 = -30$ lead to the best comparison (compare Fig.10d to Fig.9) with an almost perfect agreement.

Other parameters of the numerical model might of course impact as well this comparison. For instance, the quantity of considered streamlines might modify the hemolysis prediction. To check this issue, Fig.11 presents the influence of the number of streamlines for the best set of model parameters, when considering four times more

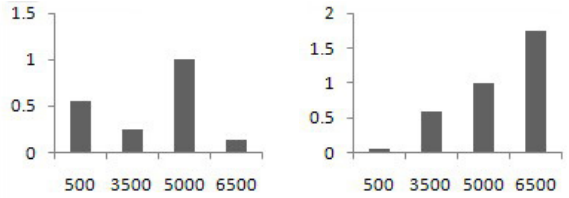

(a) $f_1 = 0.00125$, $f_2 = 0.00125$, $f_3 = -5$ (b) $f_1 = 0.01$, $f_2 = 0.0045$, $f_3 = -20$

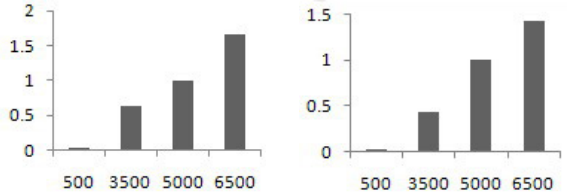

(c) $f_1 = 0.012$, $f_2 = 0.005$, $f_3 = -30$ (d) $f_1 = 0.0115$, $f_2 = 0.005$, $f_3 = -30$

Figure 10 Relative hemolysis index choosing the case with Re=5 000 **as reference (index = 1), when varying the model prefactors. Case a) corresponds to the values recommended in [4].**

streamlines in the post-processing step. The observed influence is considerably lower than that of the prefactors. However, there is a visible difference in the predicted hemolysis level, certainly associated to the fact that a varying proportion of streamlines become trapped into the recirculation zone behind the sudden expansion.

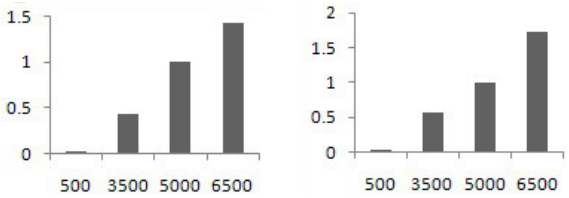

(a) $f_1 = 0.0115$, $f_2 = 0.005$, $f_3 = -30$, 869 Pathlines (b) $f_1 = 0.0115$, $f_2 = 0.005$, $f_3 = -30$, 3482 Pathlines

Figure 11 Relative hemolysis index choosing the case with Re=5 000 **as reference (index = 1), when varying the number of streamlines.**

Discussion and conclusions

The strain-based model employed in this study should be in principle far more closer to the physical properties of red blood cells than stress-based models. However, this is not sufficient to ensure that hemolysis can be directly predicted in an accurate manner. The accuracy of the corresponding CFD-based prediction is probably still case-dependent. While parameter values employed for Fig.10a performed well in [4], they give no adequate result in the sudden-expansion considered for the FDA critical path project. This is an indication that additional modeling issues must probably be taken into account before getting

an acceptable level of generality. This issue will be the subject of our future work.

After reaching this step, an optimization of the remaining model parameters might easily be carried out by comparison with reliable experimental data, as already practiced in many previous projects in our group (see for instance [10]).

Based on the experience already gained in this project, a few aspects appear already to be of high importance in order to support reliable hemolysis predictions:

1. The pathlines are essential for a high-quality analysis of hemolysis. It is therefore very important to check that the underlying numerical process is of high precision.

2. For this purpose, the volumetric mesh used for the CFD must be itself fine enough and properly resolve all the regions with high shear and rotation.

3. Comparisons have shown that, for this purpose, a structured mesh is always to be preferred if possible, with unstructured meshes introducing very large levels of errors.

4. Obviously, the quality of the CFD prediction, used as a starting point to compute hemolysis, must be checked and increased as far as possible. This means also reaching a sufficient level of convergence and using higher-order methods.

5. The numerical integration of Eq.(1) must itself be carried out with high-order and low-dissipation methods in order to get a sufficient accuracy.

After making sure that the employed hemolysis model is of sufficient accuracy and generality, it will become possible to use it in order to analyze and quantify the performance of the axial blood-pump considered in the further research project.

References

[1] D. Thévenin, G. Janiga, Optimization and Computational Fluid Dynamics, Springer (2008)

[2] M.H. Mohamed, G. Janiga, E. Pap, D. Thévenin, Multi-objective optimization of the airfoil shape of Wells turbine used for wave energy conversion. *Energy* **Vol. 36** (1), 438-446 (2011)

[3] M.H. Mohamed, G. Janiga, E. Pap, D. Thévenin, Optimal blade shape of a modified Savonius turbine using an obstacle shielding the returning blade. Energy Conversion and Management. **Vol. 52** 236-242 (2011)

[4] D. Arora, Computational hemodynamics: Hemolysis and viscoelasticity, Rice University, Ph.D. (2006)

[5] O. Coronado and D. Arora, Four-field Galerkin/least-squares formulation for viscoelastic fluids, *Journal of Non-Newtonian Fluid Mechanics* **140.1-3**, pp.132-144 (2006)

[6] S. Stewart, P. Hariharan, M. Berman, M. Myers, R. Malinauskas, Turbulence modeling as a source of error in FDA's Critical Path interlaboratory computational study of flow in a nozzle model, *American Society of Internal Artificial Organs ASAIO, 56th Annual Conference*, Poster Presentation, (2010)

[7] P. Hariharan, M. Giarra, Multilaboratory particle image velocimetry analysis of the FDA benchmark nozzle model to support validation of computational fluid dynamics simulations, *Journal of Biomechanical Engineering*, **Vol. 133**, 041002-1 (2011)

[8] S. Stewart, P. Hariharan, M. Berman, M. Myers, R. Malinauskas, , Preliminary results of FDA's "Critical Path" project to validate computational fluid dynamic methods used in medical device evaluation, *American Society of Internal Artificial Organs ASAIO, 55th Annual Conference*, Poster Presentation, (2009)

[9] S. Stewart, P. Hariharan, M. Berman, M. Myers, R. Malinauskas, Preliminary results of FDA's interlaboratory assessment of computational fluid dynamics and hemolysis in medical devices, *FDA / NHLBI / NSF Workshop on Computer Methods for Cardiovascular Devices*, Poster Presentation, (2009)

[10] T. Chittipotula, G. Janiga, D. Thévenin, Optimizing soot prediction models for turbulent non-premixed ethylene/air flames. *Chemical Engineering Science*, in press (2011)